

University of Nebraska - Lincoln

DigitalCommons@University of Nebraska - Lincoln

Biological Systems Engineering: Papers and Publications

Biological Systems Engineering

2016

Cellulase immobilization on superparamagnetic nanoparticles for reuse in cellulosic biomass conversion

Qing Song


Yu Mao

Mark Wilkins

Fernando Segato

Rolf Prade

Follow this and additional works at: <https://digitalcommons.unl.edu/biosysengfacpub>

 Part of the [Bioresource and Agricultural Engineering Commons](#), [Environmental Engineering Commons](#), and the [Other Civil and Environmental Engineering Commons](#)

This Article is brought to you for free and open access by the Biological Systems Engineering at DigitalCommons@University of Nebraska - Lincoln. It has been accepted for inclusion in Biological Systems Engineering: Papers and Publications by an authorized administrator of DigitalCommons@University of Nebraska - Lincoln.



Research article

Cellulase immobilization on superparamagnetic nanoparticles for reuse in cellulosic biomass conversion

Qing Song¹, Yu Mao^{2,*}, Mark Wilkins², Fernando Segato³, and Rolf Prade³

¹ Department of Immunology, Institute of Tuberculosis Control, Institute of Human Virology, Zhongshan School of Medicine, Sun Yat-sen University, Guangzhou 510080, China; Key Laboratory of Tropical Diseases Control (Sun Yat-sen University), Ministry of Education, Guangzhou 510080, China

² Department of Biosystems Engineering, Oklahoma State University, Stillwater, OK 74078, USA

³ Department of Microbiology and Molecular Genetics, Oklahoma State University, Stillwater, OK 74078, USA

* **Correspondence:** Email: yu.mao@okstate.edu; Tel: +1-405-744-4337; Fax: +1-405-744-6059.

Abstract: Current cellulosic biomass hydrolysis is based on the one-time use of cellulases. Cellulases immobilized on magnetic nanocarriers offer the advantages of magnetic separation and repeated use for continuous hydrolysis. Most immobilization methods focus on only one type of cellulase. Here, we report co-immobilization of two types of cellulases, β -glucosidase A (BglA) and cellobiohydrolase D (CelD), on sub-20 nm superparamagnetic nanoparticles. The nanoparticles demonstrated 100% immobilization efficiency for both BglA and CelD. The total enzyme activities of immobilized BglA and CelD were up to 67.1% and 41.5% of that of the free cellulases, respectively. The immobilized BglA and CelD each retained about 85% and 43% of the initial immobilized enzyme activities after being recycled 3 and 10 times, respectively. The effects of pH and temperature on the immobilized cellulases were also investigated. Co-immobilization of BglA and CelD on MNPs is a promising strategy to promote synergistic action of cellulases while lowering enzyme consumption.

Keywords: enzyme co-immobilization; β -glucosidase; cellobiohydrolase; superparamagnetic nanoparticles; cellulase reuse

Abbreviations

APTES (3-aminopropyl) triethoxysilane

BglA	β -glucosidase A
CelD	cellobiohydrolase D
FTIR	Fourier transform infrared spectroscopy
MNPs	magnetic nanoparticles
PBS	phosphate buffer saline
pNPG	4-nitrophenyl- β -D-glucopyranoside
pNPC	4-nitrophenyl- β -D-cellobioside
pNP	p-nitrophenol
RT	room temperature
TEM	transmission electron microscope

1. Introduction

Cellulosic biomass, serving as a renewable carbon and energy source, provides a significantly large amount of feedstock for producing sugars. These sugars can be biochemically converted into desired metabolites, such as lactic acid, succinic acid, and levulinic acid, or biofuel, such as ethanol and butanol [1]. The polysaccharide cellulose is composed of a linear chain of abundant $\beta(1\rightarrow4)$ linked D-glucose units [2]. Cellulose can be decomposed into glucose by the synergistic action of three types of enzymes: endo-glucanase, cellobiohydrolase, and β -glucosidase [3]. Endo-glucanase randomly breaks internal bonds of amorphous cellulose to expose individual cellulose polysaccharide chains. Cellobiohydrolase cleaves 2–4 units from the end of the exposed chains, producing tetrasaccharides and disaccharides such as cellobiose. β -glucosidase hydrolyses cellobiose into glucose [3]. These cellulases are produced by various bacteria, fungi, and plants [1].

Due to the mechanism of product inhibition, accumulation of glucose restrains the activity of β -glucosidase, and accumulation of cellobiose impedes the activities of cellobiohydrolase and endo-glucanase [4], which adversely affects sugar production. The current solution for product inhibition is to add more cellulases during biomass hydrolysis, which inevitably results in the increase of production cost [5]. Enzyme immobilization enables enzyme separation from products for recycling and reuse of cellulases, thus reducing enzyme consumption [6]. Immobilization may change enzyme structure and diminish the effects of product inhibition [7]. In addition, immobilized enzymes often possess preferable operational, storage, and temperature stabilities compared with free enzymes [6]. Cellulases have been physically adsorbed on supports or entrapped within gel matrices [8]. These physical immobilization methods have advantages in retaining the enzyme activity, but they usually result in the leaking of enzymes [8]. Cellulases can also be immobilized on carriers through covalent bonds, which significantly alleviate the leaking problem [8]. Several carriers have been employed to covalently immobilize cellulases, such as cyanogen bromide-activated agarose [9], nylon [10], and liposome [11].

Recently, covalent immobilization of cellulase on magnetic nanoparticles (MNPs) has attracted increasing attention, because MNPs can be easily separated using an external magnetic field. In addition, the high surface area to volume ratio of nanoparticles enlarges anchoring areas of enzymes and enhances catalytic reaction [12]. Immobilization of one type cellulase on MNPs has been reported. For example, cellobiase (also called β -glucosidase) immobilized on core-shell MNPs demonstrated improved stability at high temperature and low pH compared with free cellobiase [13].

In another study, β -glucosidase covalently bound on iron oxide nanoparticles displayed enhanced thermostability compared to free β -glucosidase and exhibited excellent recyclability [14].

For effective enzymatic hydrolysis of cellulose, at least two different enzyme activities are required. Endoglucanase randomly attacks glycosidic bonds in cellulose while cellobiohydrolase cleaves the dimer cellobiose from non-reducing ends of cellulose and β -glucose oligomers formed by the action of endoglucanase [15]. Cellobiose is then hydrolyzed to produce glucose by β -glucosidase [16]. At a minimum, cellobiohydrolase and β -glucosidase activities are required to produce glucose from cellulose. Immobilization of only one cellulase type does not provide the synergistic function required for cellulose hydrolysis to glucose.

In this study, we demonstrate simultaneous immobilization of cellobiohydrolase D (CelD) and β -glucosidase A (BglA) on sub-20 nm superparamagnetic nanoparticles (Figure 1). The enzyme activity, effects of temperature and pH, thermostability, and pH-dependent stability of the immobilized CelD and BglA were systematically investigated. The reusability of immobilized CelD and BglA were also studied.

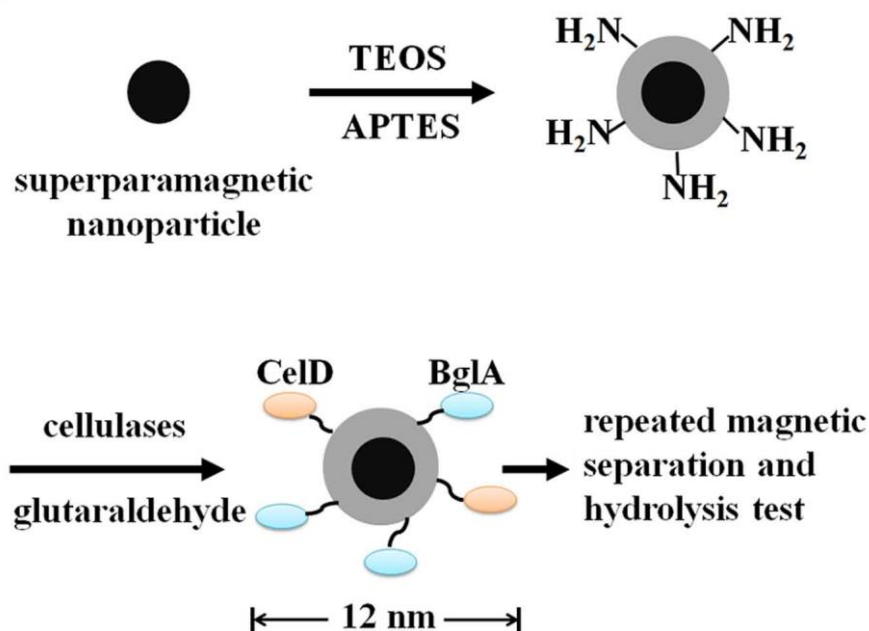


Figure 1. Co-immobilization of both CelD and BglA on superparamagnetic nanoparticles.

2. Materials and Method

2.1. Materials

Diethylene glycol (99%) and ferric chloride (>98%) were obtained from Alfa Aesar (Ward Hill, MA, USA). Ferrous chloride (>99%) and tetraethyl orthosilicate (TEOS, 98%) were from Acros Organics (Fair Lawn, NJ, USA). (3-aminopropyl) triethoxysilane (APTES, 99%), 4-nitrophenyl- β -D-glucopyranoside (pNPG, >98%), 4-nitrophenyl- β -D-cellobioside (pNPC, >98%),

p-nitrophenol (pNP, >99%), sodium acetate (>99%), and sodium carbonate (>99%) were purchased from Sigma-Aldrich (St. Louis, MO, USA). Glutaraldehyde (50%) was ordered from Electron Microscopy Sciences (Hatfield, PA, USA). Ammonia (28–30% NH₃) was obtained from Pharmco-AAPER (Brookfield, CT, USA). Phosphate buffer (PBS, pH 7.4) and sodium hydroxide (>97%) were purchased from Fisher Scientific (Denver, CO, USA). McIlvaine's buffer was obtained from LabChem (Zelienople, PA, USA). The protein assay kit was ordered from Bio-Rad (Hercules, CA, USA).

2.2. Preparation of cellobiohydrolase (CelD) and β -glucosidase (BglA)

Cellobiohydrolase D (CelD) and β -glucosidase A (BglA) were produced by the *Aspergillus nidulans* pEXPYR cell factory system [17]. Briefly, the genes (ORF) for CelD (AN0494) and BglA (AN4102) were cloned into pEXPYR expression and secretion vector [17] and transformed into *A. nidulans* A773 (pyrG, wA, pyroA4). Recombinant strains were used to produce CelD and BglA. 10⁷–10⁸ spores/mL were inoculated in liquid minimal medium supplemented with 0.5 to 2.5% maltose, distributed onto dishes (10 mL in 60 mm, 20 mL in 150 mm Petri-dishes and 500 mL onto cafeteria trays) and incubated (stationary) at 37 °C for 2 days. The mycelial mat was lifted with a spatula and discarded and the medium was collected by filtration, centrifuged at 10,000 g for 10 min prior to concentration by ultra-filtration (10,000 dalton cutoff Amicon), quantified by the Bradford method [18], validated for purity by SDS PAGE [19] and used for biochemical studies.

2.3. Synthesis of MNPs

Naked MNPs were first synthesized in diethylene glycol [20]. Two mmol FeCl₂ 4H₂O and 4 mmol FeCl₃ were dissolved in 80 g of diethylene glycol in a Schlenk flask under protection of nitrogen gas at 150 °C. Next, 16 mmol NaOH was dissolved in 40 g of diethylene glycol and added to the solution of metal chlorides while stirring. The mixture was heated to 210–220 °C for 4 h for the formation of naked MNPs. After the reaction mixture was washed with ethanol twice using a centrifuge at 10,000 rpm for 8 min, deionized water was added to dissolve the naked MNPs. The second step was to modify the MNP surface with silica. Briefly, 170 mg naked MNPs in deionized water were added into a Schlenk flask with 40 mL of ethanol and 6 mL of deionized water. One mL NH₄OH and 0.1 mL TEOS were added into the reaction system and reacted for 6 h at room temperature (RT) to form silica shell on MNPs. The third step was to modify the silica MNPs with primary amine groups. One mL NH₄OH and 0.01 mL APTES were injected into the reaction system with silica MNPs and stirred for 1 h at RT. The temperature was subsequently increased to 90 °C for another hour [21]. Finally, the primary amine group functionalized MNPs were centrifuged, purified, and dissolved in deionized water.

2.4. Immobilization of cellulases

500 μ L MNPs with primary amine groups were incubated in 10 mL 5% (v/v) glutaraldehyde in 0.1 M PBS for 6 h at RT. The mixture was washed 5 times with 0.1 M PBS and dissolved in 1 mL deionized water. Next, 50 μ L MNPs with glutaraldehyde were incubated with 100 μ L enzyme in 800 μ L of 0.1 M PBS overnight. The amount of enzyme was chosen to achieve the optimal

immobilized enzyme density based on the results pre-experiments. At last, the MNPs bound with enzymes were washed 4 times with deionized water to remove free enzymes and finally dissolved in deionized water.

2.5. Characterizations

Both naked MNPs and MNPs after cellulase immobilization were observed using a JEOL JEM 100CX II transmission electron microscope (TEM) to quantify the particle dimension. The average diameter of MNPs was measured and calculated. Fourier transform infrared (FTIR) spectra of the MNPs before and after cellulase immobilization were collected by a Nicolet 6700 FTIR spectrometer using a DTGS detector under the transmission mode at a 4 cm^{-1} resolution. The amount of protein immobilized was determined by measuring the protein contents in the solution after immobilization using the Bio-Rad protein assay kit. The method was used with bovine serum albumin as the standard.

2.6. Enzyme activity assay

BglA and CelD activities were measured using the hydrolysis of pNPG (0.25%) and pNPC (0.25%) in a sodium acetate buffer (50 mM, pH 5.0), respectively. After reacting for 30 min at $42\text{ }^{\circ}\text{C}$, the MNPs with cellulases immobilized were separated by a magnetic field of around 100 Gauss (measured by a Gauss meter). The pNP was measured using an Infinite 200 PRO Nanoquant UV-Vis spectrometer (Tecan) at 400 nm after adding Na_2CO_3 solution (0.3 M) at the same volume. The pNP concentration was calculated from a pNP standard curve. The activity of free enzymes was also measured, and the relative activity of the immobilized enzyme was calculated using the ratio of the specific activity of the immobilized enzyme to that of the free enzyme.

2.7. Reusability assay

The reusability of the immobilized cellulases was examined by repeatedly measuring the enzyme activities at $42\text{ }^{\circ}\text{C}$ for 30 min. After each cycle of reaction, the immobilized enzymes were magnetically separated and washed twice with 0.1 M PBS. The activities of immobilized enzymes were then measured in the next cycle. All assays were done in triplicate.

2.8. pH optimum, pH-dependent stability, temperature optimum, and thermostability measurement

The effect of pH on cellulase activities was evaluated over a pH range of 3.0–8.0 using McIlvaine's buffer. The enzymes were first incubated in McIlvaine's buffer systems (pH 3.0, 4.0, 4.4, 5.0, 5.4, 6.0, 7.0 and 8.0) in the absence of substrates for 2.5 h. Then, the incubated enzymes were subjected to the enzyme activity assay at $42\text{ }^{\circ}\text{C}$ for the measurement of pH-dependent stability. The optimal temperatures of BglA and CelD were measured by performing the enzyme activity assay at temperatures ranging from 4 to $75\text{ }^{\circ}\text{C}$ in a sodium acetate buffer (50 mM, pH 5.0). The thermostability of enzymes was investigated after incubating at temperatures of 4, 35, 45, 55, 65, and $75\text{ }^{\circ}\text{C}$ for 2.5 h followed by enzyme activity assay at $42\text{ }^{\circ}\text{C}$. All assays were conducted in triplicate. Statistical analysis was performed by one-way ANOVA followed by Tukey's HSD test, using

GraphPad Prism 5 (GraphPad Software, La Jolla, CA, USA). $P < 0.05$ was considered to be statistically significant.

3. Results and Discussion

3.1. MNP properties

The average diameter of the naked MNPs was measured to be 7.7 nm based on TEM (Figure 2a), which was smaller than the superparamagnetic critical size of iron oxide particles (20 nm) [22]. Therefore, the MNPs exhibited superparamagnetic characteristics, which means that the MNPs magnetize up to their saturation magnetization in the presence of an external magnetic field, but they do not retain any residual magnetic moment in the absence of a magnetic field [23]. The MNPs were observed to be easily separated from an aqueous solution by a magnetic field of 100 Gauss created by a magnetic bar within 1 min, and upon the removal of the magnetic field, the MNPs were quickly re-dispersed into the aqueous solution, which facilitated recycling and reuse of MNPs. After the hydrolysis of TEOS [21] on the surface of naked MNPs, silica MNPs were formed with an iron oxide core and an amorphous silica shell. The silica MNPs were dispersible in water, most likely due to the negative charges on the silica shell surfaces [21].

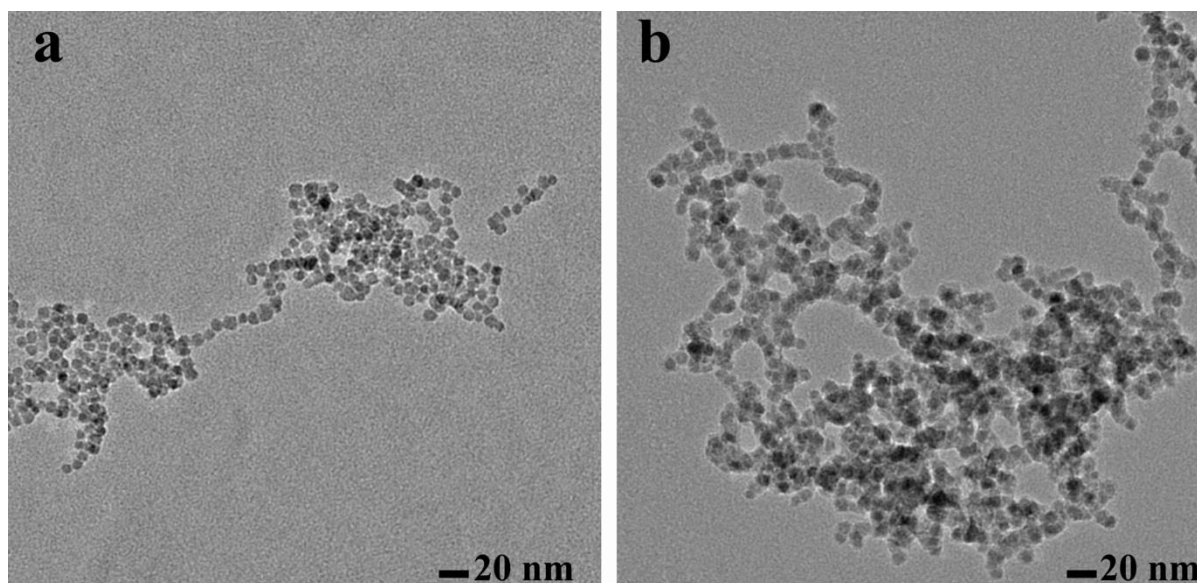


Figure 2. TEM images of (a) iron oxide nanoparticles and (b) silica MNPs bound with cellulases.

3.2. Enzyme immobilization

After the cellulase immobilization on silica MNPs, the MNP average diameter increased to 11.5 nm, as measured by TEM (Figure 2b). New absorption peaks appeared in the spectrum of silica MNPs after cellulase immobilization, as shown in Figure 3. The peak around 1648.4 cm^{-1} was attributed to absorption of the enzyme amide I [24]. The band centered at 1541.2 cm^{-1} was attributed to the amide II of enzymes due to the coupling of NH-bending with CN stretching [25]. The

aforementioned peaks confirmed the covalent immobilization of enzymes on the MNPs. Other absorption peaks were attributed to the magnetite core and the silica shell. The peak at 568.6 cm^{-1} was due to the vibrations of Fe-O bond [26]. The strong absorption around 1077.0 cm^{-1} was ascribed to the Si-O-Si stretching. The peak at 1633.4 cm^{-1} was assigned to the bending of free water [27] that remained in MNPs. The broad band in the range of $3000\text{--}3600\text{ cm}^{-1}$ was due to -OH groups [24].

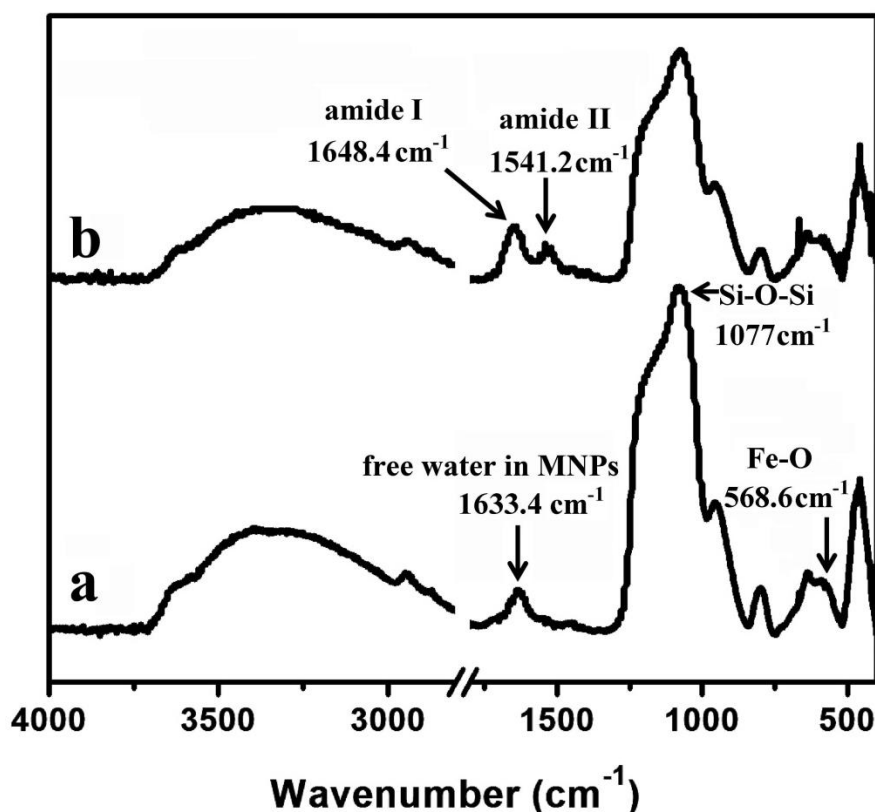


Figure 3. FTIR spectra of silica MNPs (a) before and (b) after cellulase immobilization.

After enzyme immobilization, the concentration of proteins that remained in the solution was measured. It is interesting that no enzyme was observed in the solution using the Bio-Rad protein assay. The 100% immobilization efficiency for both BglA and CelD was attributed to the high surface area to volume ratio of sub-20 nm MNPs, which significantly increased enzyme anchoring areas and further improved enzymatic catalysis [12]. Based on the measurement of the MNP dry weight and the original enzyme quantity, the enzyme immobilization loading was calculated to be 6.4 mg protein/g MNPs.

The enzyme activities of free BglA and CelD was quantified to be 43.4 and $12.0\text{ }\mu\text{mol min}^{-1}$ $(\text{mg protein})^{-1}$, respectively. The enzyme activities of immobilized BglA and CelD were $67.1 \pm 1.2\%$ and $41.5 \pm 2.7\%$ of the activities of the free BglA and CelD, respectively. It is possible that the glutaraldehyde reaction might change the enzyme structure and alter the conformation of the enzyme catalytic center. In addition, immobilization restricts enzyme movement [28], which may reduce enzyme activity as well. The β -glucosidase immobilized on iron oxide nanoparticles was reported to demonstrate 73% of free β -glucosidase activity [29], and cellulase immobilized on a silica gel demonstrated only 7% of free cellulase activity [28]. Although covalent immobilization decreased

enzyme activity, this method prevented enzyme leaching out into the surroundings and eliminated protein contamination in the product [6]. Additionally, the deficiency of reduced enzyme activity can be mitigated by the reutilization of immobilized enzymes.

3.3. Reusability assay of immobilized BglA and CelD

The reusability of immobilized cellulases was measured using up to 10 cycles of 30 min. After three cycles, the remaining activities of the immobilized BglA and CelD were 84.1% and 85.3% of the initial enzyme activity, respectively. After 10 cycles, the remaining activities were 43.3% and 43.4% for immobilized BglA and CelD, respectively (Figure 4). It is interesting to note that our immobilized BglA and CelD demonstrated similar remaining activities after each reuse, possibly due to the co-anchoring of two cellulases on the same MNPs at the same conditions. On the other hand, the remaining activities of single-type immobilized cellulases varied under different reaction conditions. For example, immobilized cellulase retained about 70% and 32% of initial activity after 3 and 10 cycles of 30 min, respectively [30], and immobilized β -glucosidase retained approximately 50% of initial activity after 16 cycles of 10 min [14]. Although enzyme activities of immobilized cellulases decreased with the increase of recycle times, reutilization and recycling of cellulases reduce the overall amount of fresh enzyme that needs to be used over time.

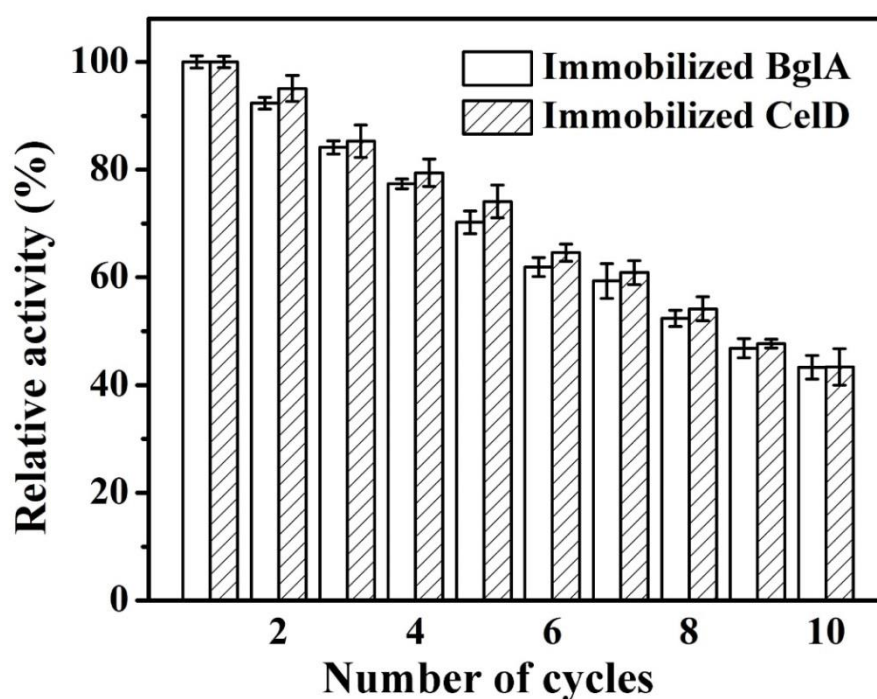


Figure 4. Reusability of immobilized BglA and CelD. Relative activity is expressed as the percentage of the residual activity compared to the initial activity.

3.4. Effects of pH on free and immobilized cellulases

Based on statistical analysis, the optimum pH of the free and immobilized BglA was 5.4 ($p < 0.05$, Figure 5a) in the McIlvaine's buffer systems. Free CelD had a wider optimum pH range (from

pH 4.4 to 5.0) than immobilized CelD (pH 5.0) (Figure 5b). The pH-dependent stabilities of free and immobilized BglA and CelD are shown in Figures 5c and 5d, respectively. The activities of both free and immobilized enzymes decreased significantly after 2.5 h incubation in buffers with different pH. The highest remaining activities were 57% and 46% for free and immobilized BglA, respectively. For free and immobilized CelD, the highest remaining activities were 32% and 29%, respectively. Free BglA was more stable than immobilized BglA in the pH range from 4.4 to 7.0 ($p < 0.05$), while there was no significant difference between free and immobilized BglA at pH 3.0, 4.0, and 8.0 ($p > 0.05$), indicating that immobilized BglA was more sensitive to pH variation from pH 4.4 to 7.0. Immobilized CelD was found to be more stable than free CelD at pH 3.0 ($p < 0.05$), while no significant differences were observed from pH 4.0 to 8.0 ($p > 0.05$) except at pH 6.0 ($p < 0.05$). It is noted that the enzyme optimum pH is different from the most stable pH, as observed in other studies [31]. For example, the optimum pH of immobilized BglA was 5.4, while its most stable pH was 7.0. The most stable pHs of the free BglA (pH 7.0) and CelD (pH 5.0 to 6.0) were different than their optimum pHs as well.

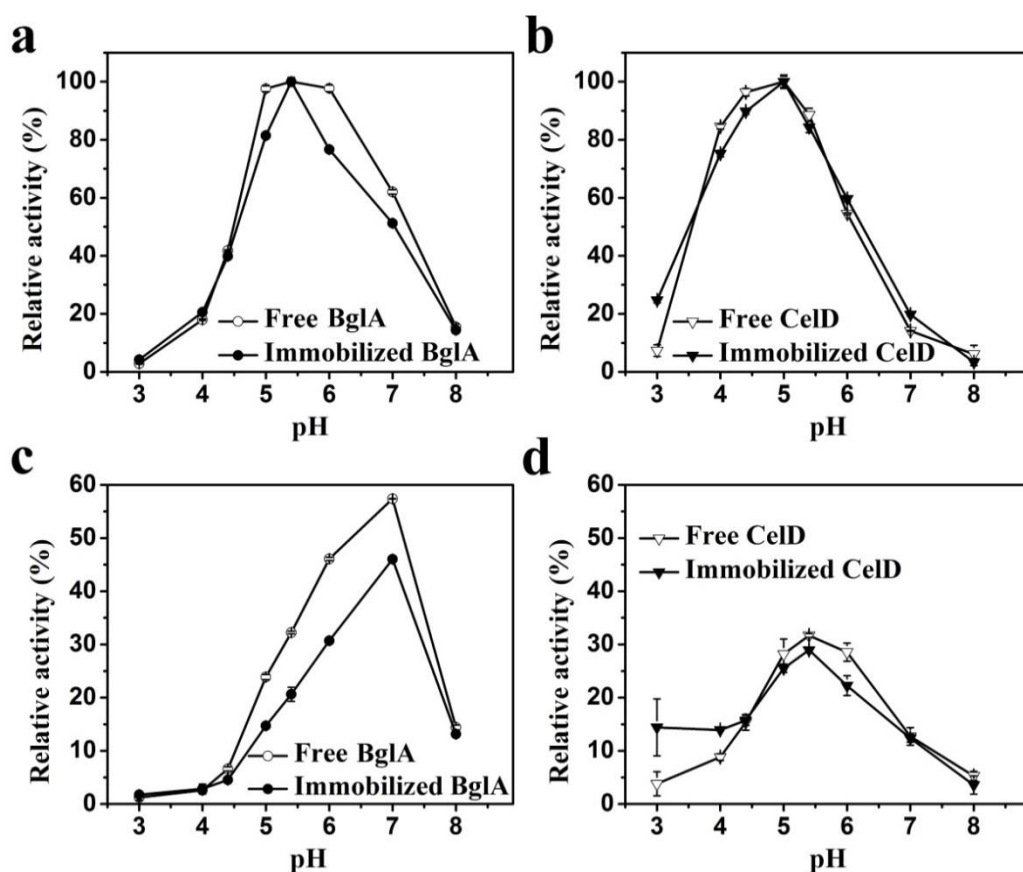


Figure 5. Effects of hydrolysis pH on the activity of (a) BglA and (b) CelD, relative activity is expressed as the percentage of the residual activity compared to the highest enzyme activity at optimum pH; pH-dependent stability of (c) BglA and (d) CelD, relative activity is expressed as the percentage of the residual activity compared to the initial enzyme activity before incubation.

3.5. Effects of temperature on free and immobilized cellulases

The activities of the free and immobilized enzymes at different temperatures were measured while maintaining pH at 5.0. Both immobilized enzymes had a wider optimum temperature range from 55 °C to 65 °C than free enzymes, as shown in Figures 6a and 6b. The relative enzyme activities of immobilized BglA were higher than those of free BglA over most of the temperature points, suggesting that immobilized BglA had more preferable temperature adaptability than free BglA. In Figure 6c, thermostability of immobilized BglA was higher than free BglA after incubation at 35 °C and 45 °C ($p < 0.05$), and the corresponding activities were 111% and 116% of the initial activity of immobilized BglA. This indicated that immobilized BglA had better heat resistance than free BglA at 35 °C and 45 °C. Thermostability of immobilized CelD was not superior to free CelD. Covalent immobilization may change cellulase conformation, resulting in different activities and stability towards pH and temperature compared with free cellulases [14,30]. These obtained temperature and pH data of immobilized BglA and CelD will be of benefit for practical applications of these two types of immobilized cellulases during independent or synergistic catalyzing process. In synergistic action, consideration of the optimum reaction conditions should be given to the overall balance of BglA and CelD characteristics, which plays an important role in promoting production efficiency of decomposing cellulose into fermentable sugars.

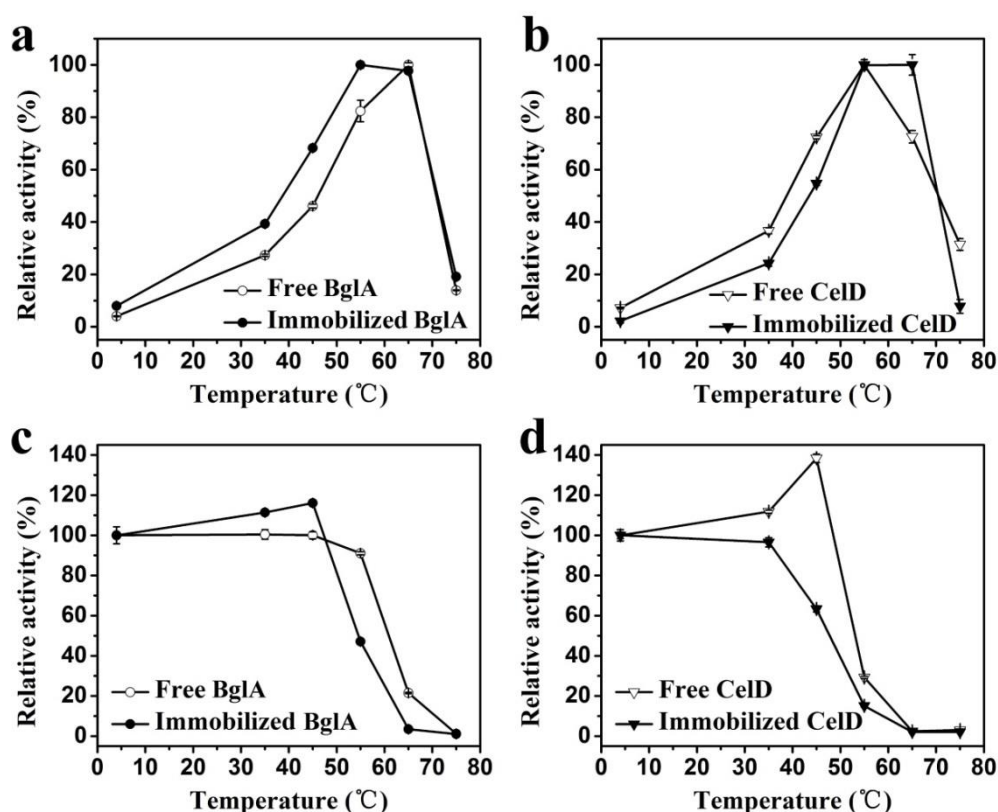


Figure 6. Effect of temperature on the relative activity of (a) BglA and (b) CelD, relative activity is expressed as the percentage of the residual activity compared to the highest enzyme activity at optimum temperature; thermostability of (c) BglA and (d) CelD, relative activity is expressed as the percentage of the residual activity compared to the initial enzyme activity before incubation.

4. Conclusion

CelD and BglA were covalently co-immobilized on superparamagnetic nanoparticles (MNPs). MNPs demonstrated 100% immobilization efficiency for both cellulases. Immobilized cellulases could be quickly separated using a magnetic field of 100 Gauss, and they retained about 85% and 43% of the initial activities after 3 and 10 reuses, respectively. Both immobilized BglA and CelD had a wider optimum temperature range than the non-immobilized counterparts, and the immobilized BglA exhibited better thermostability at 35 °C and 45 °C. The co-immobilization of cellulases on MNPs has the potential to significantly reduce enzyme use and benefits the synergistic action of cellulases during sugar production.

Acknowledgments

Financial support for this research was provided by the Oklahoma Center for the Advancement of Science and Technology (Grant number AR11-044) and the Department of Transportation South Central Sun Grant Initiative. We also thank Dr. Andrew Mort, Dr. Michael Mueller, Tong Liu, Jian Liu, Rosymar C. de Lucas, Siamak Dadras, and Xiangmei Wu for their help during experiments.

Conflict of Interest

All authors declare no conflict of interest in this paper.

References

1. Menon V, Rao M (2012) Trends in bioconversion of lignocellulose: Biofuels, platform chemicals & biorefinery concept. *Prog Energy Combust Sci* 38: 522–550.
2. Wang H, Gurau G, Rogers RD (2012) Ionic liquid processing of cellulose. *Chem Soc Rev* 41: 1519–1537.
3. Bhat M, Bhat S (1997) Cellulose degrading enzymes and their potential industrial applications. *Biotechnol Adv* 15: 583–620.
4. Lynd LR, Weimer PJ, van Zyl WH, et al. (2002) Microbial cellulose utilization: fundamentals and biotechnology. *Microbiol Mol Biol Rev* 66: 506–577.
5. Lee SM, Jin LH, Kim JH, et al. (2010) β -glucosidase coating on polymer nanofibers for improved cellulosic ethanol production. *Bioprocess Biosyst Eng* 33: 141–147.
6. Sheldon RA (2007) Enzyme immobilization: the quest for optimum performance. *Adv Synth Catal* 349: 1289–1307.
7. Mateo C, Palomo JM, Fernandez-Lorente G, et al. (2007) Improvement of enzyme activity, stability and selectivity via immobilization techniques. *Enzyme Microb Technol* 40: 1451–1463.
8. Mohamad NR, Marzuki NHC, Buang NA, et al. (2015) An overview of technologies for immobilization of enzymes and surface analysis techniques for immobilized enzymes. *Biotechnol Biotechnol Equip* 29: 205–220.
9. Chim-Anage P, Kashiwagi Y, Magae Y, et al. (1986) Properties of cellulase immobilized on agarose gel with spacer. *Biotechnol Bioeng* 28: 1876–1878.

10. Isgrove F, Williams R, Niven G, et al. (2001) Enzyme immobilization on nylon-optimization and the steps used to prevent enzyme leakage from the support. *Enzyme Microb Technol* 28: 225–232.
11. Li C, Yoshimoto M, Fukunaga K, et al. (2007) Characterization and immobilization of liposome-bound cellulase for hydrolysis of insoluble cellulose. *Bioresour Technol* 98: 1366–1372.
12. Georgelin T, Maurice V, Malezieux B, et al. (2010) Design of multifunctionalized γ -Fe₂O₃@SiO₂ core-shell nanoparticles for enzymes immobilization. *J Nanopart Res* 12: 675–680.
13. Wang P, Hu X, Cook S, et al. (2009) Influence of silica-derived nano-supporters on cellobiase after immobilization. *Appl Biochem Biotechnol* 158: 88–96.
14. Verma ML, Chaudhary R, Tsuzuki T, et al. (2013) Immobilization of β -glucosidase on a magnetic nanoparticle improves thermostability: Application in cellobiose hydrolysis. *Bioresour Technol* 135: 2–6.
15. Wood TM, Bhat KM (1988) Methods for measuring cellulase activities. *Methods Enzymol* 160: 87–112.
16. Saha BC, Bothast RJ (1996) Production, purification, and characterization of a highly glucose-tolerant novel beta-glucosidase from *Candida peltata*. *Appl Environ Microbiol* 62: 3165–3170.
17. Segato F, Damásio AR, Gonçalves TA, et al. (2012) High-yield secretion of multiple client proteins in *Aspergillus*. *Enzyme Microb Technol* 51: 100–106.
18. Bradford MM (1976) A rapid and sensitive method for the quantitation of microgram quantities of protein utilizing the principle of protein-dye binding. *Anal Biochem* 72: 248–254.
19. Shapiro AL, Viñuela E, Maizel JV Jr (1967) Molecular weight estimation of polypeptide chains by electrophoresis in SDS-polyacrylamide gels. *Biochem Biophys Res Commun* 28: 815–820.
20. Caruntu D, Caruntu G, Chen Y, et al. (2004) Synthesis of variable-sized nanocrystals of Fe₃O₄ with high surface reactivity. *Chem Mater* 16: 5527–5534.
21. Lu Y, Yin Y, Mayers BT, et al. (2002) Modifying the surface properties of superparamagnetic iron oxide nanoparticles through a sol-gel approach. *Nano Lett* 2: 183–186.
22. Caruntu D, Caruntu G, O'Connor CJ (2007) Magnetic properties of variable-sized Fe₃O₄ nanoparticles synthesized from non-aqueous homogeneous solutions of polyols. *J Phys D Appl Phys* 40: 5801–5809.
23. Wahajuddin, Arora S (2012) Superparamagnetic iron oxide nanoparticles: magnetic nanoplatforms as drug carriers. *Int J Nanomedicine* 7: 3445–3471.
24. Kannan K, Jasra RV (2010) Improved catalytic hydrolysis of carboxy methyl cellulose using cellulase immobilized on functionalized meso cellular foam. *J Porous Mat* 18: 409–416.
25. Jung C (2000) Insight into protein structure and protein-ligand recognition by Fourier transform infrared spectroscopy. *J Mol Recognit* 13: 325–351.
26. Gotić M, Musić S (2007) Mössbauer, FT-IR and FE SEM investigation of iron oxides precipitated from FeSO₄ solutions. *J Mol Struct* 834: 445–453.
27. Gai L, Li Z, Hou Y, et al. (2010) Preparation of core-shell Fe₃O₄/SiO₂ microspheres as adsorbents for purification of DNA. *J Phys D Appl Phys* 43: 5625–5634.
28. Zhang D, Hegab HE, Lvov Y, et al. (2016) Immobilization of cellulase on a silica gel substrate modified using a 3-APTES self-assembled monolayer. *Springerplus* 5: 48.

29. Zhou J, Zhang J, Gao W (2014) Enhanced and selective delivery of enzyme therapy to 9L-glioma tumor via magnetic targeting of PEG-modified, β -glucosidase-conjugated iron oxide nanoparticles. *Int J Nanomedicine* 9: 2905–2917.
30. Abraham RE, Verma ML, Barrow CJ, et al. (2014) Suitability of magnetic nanoparticle immobilised cellulases in enhancing enzymatic saccharification of pretreated hemp biomass. *Biotechnol Biofuels* 7: 90–101.
31. Ladeira SA, Cruz E, Delatorre AB, et al. (2015). Cellulase production by thermophilic *Bacillus* sp. SMIA-2 and its detergent compatibility. *Electron J Biotechnol* 18: 110–115.



AIMS Press

© 2016 Yu Mao, et al., licensee AIMS Press. This is an open access article distributed under the terms of the Creative Commons Attribution License (<http://creativecommons.org/licenses/by/4.0>)